Supplemental Figure 1

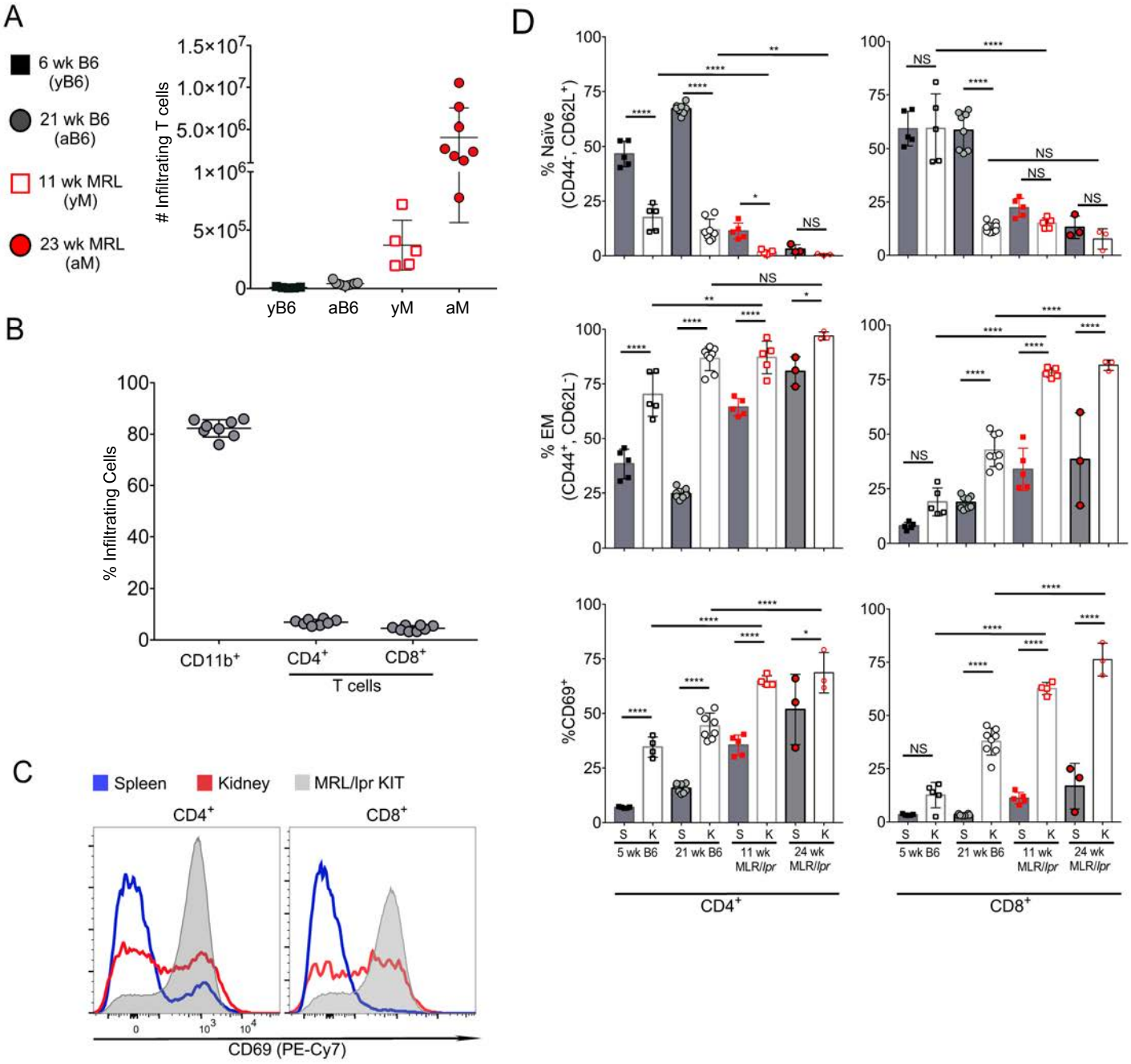

Supplemental Figure 1: Phenotypic Characterization of KITs from B6 and young MRL/*lpr* mice.

(A) Number of T cells (TCRβ$^+$) isolated from the kidneys of indicated mouse strains at indicated ages was determined using flow cytometry. Each dot represents an individual mouse, horizontal lines represent the mean and error bars show 1 standard deviation.

(B) The frequency of CD11b$^+$ and TCRβ$^+$ populations (CD4$^+$, CD8$^+$) in kidney infiltrates obtained from 5 month old B6 mice was determined using flow cytometry (n=8). Each dot denotes an individual mouse, horizontal lines represent the mean and error bars show 1 standard deviation.

(C) Representative histogram of CD69 expression on CD4$^+$ and CD8$^+$ T cells from indicated organs (blue = spleen, red = kidney) from 5 month old B6 mice. Grey histograms represent MRL/*lpr* KITs.

(D) Summary data comparing splenic T cells (grey bars: S) and KITs (white bars: K) from young (6 wk) or aged (21 week) B6 T and young (11 wk) or aged (24 wks) MRL/*lpr* mice. CD4$^+$ (left column) and CD8$^+$ T cells (right column) are depicted, showing summaries for: naive T cells (TCR$^+$ CD62L^{high}, CD44^{low}), effector memory (TCR$^+$ CD62L^{low}, CD44^{high}) or CD69$^+$ T cells (TCR$^+$ CD69$^+$). For tabulated data each dot denotes an individual mouse with bars representing the mean and error bars showing 1 standard deviation. Young B6 (n=5), old B6 (n=9), young MRL/*lpr* (n=5), old MRL/*lpr* (n=3) represent mice combined from several experiments in a single analysis. ANOVA with Tukey's multiple comparison test was used to determine statistical significance between spleen and kidney samples (* $p<0.05$, ** $p<0.01$, *** $p<0.001$,**** $p<0.0001$).

Supplemental Figure 2

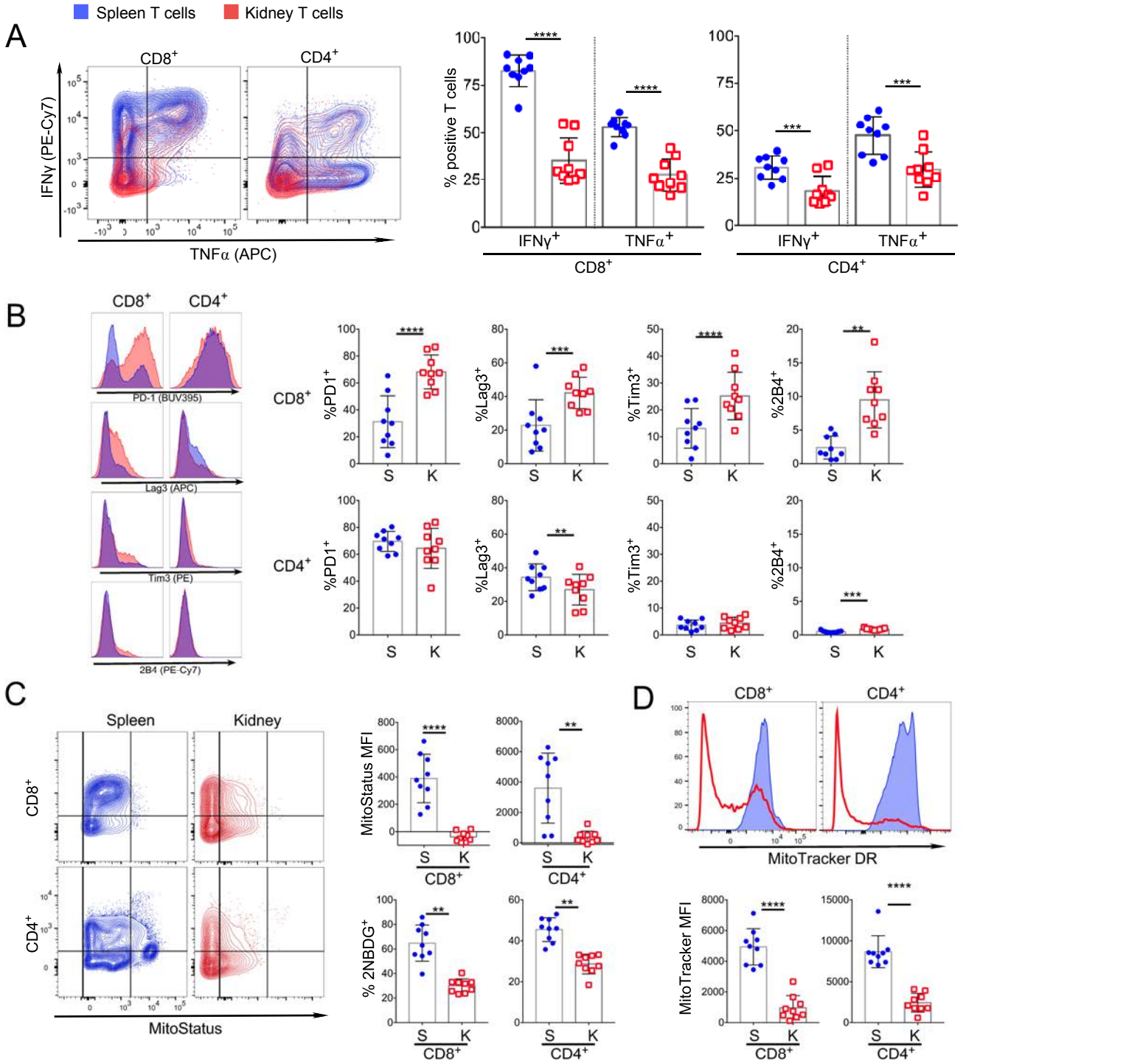

Supplemental Figure 2. **Supplemental Figure 2**. MRL.*Tlr9*$^{-/-}$ KITs recapitulate features observed in MRL/*lpr* KITs.

(A) T cells were isolated from the kidney (red) and spleen (blue) of nephritic MRL. *Tlr9*$^{-/-}$mice. Cells were stimulated in bulk culture with PMA and ionomycin in the presence of brefeldin A for 4 hours and TNFα and IFNγ cytokine expression was assessed by flow cytometry. Shown are representative contour plots depicting cytokine production by CD4$^+$ and CD8$^+$ T cells and associated tabulated data represented in the left panels.

(B) Representative histograms of IR expression on CD8$^+$ and CD4$^+$ T cells from kidney (red) and spleen (blue) derived from MRL.*Tlr9*$^{-/-}$ mice. Tabulated data are presented as dots for individual mice.

(C) Representative contour plots of MRL.*Tlr9*$^{-/-}$ splenic- or kidney-derived CD8$^+$ (upper panel) and CD4$^+$ (lower panel) T cells showing 2-NBDG (glucose uptake) and MitoStatus (mitochondrial membrane potential) staining. Tabulated data are presented for MitoStatus MFI and % positive cells for 2-NBDG.

(D) Mitochondrial mass was assessed by flow cytometry using MitoTracker DR. Representative histograms (red: kidney and blue: spleen) of MitoTracker DR from T cell lineages as indicated from MRL.*Tlr9*$^{-/-}$ mice with summary data in dot plots (below).

For tabulated data, each dot denotes an individual mouse and bars represent the mean with error bars indicating standard deviation (n=9 per group). Paired Student's t test was used to determine statistical significance between spleen and kidney samples (* p<0.05, **p<0.01, ***p<0.001, **** p<.0001).

Supplemental Figure 3

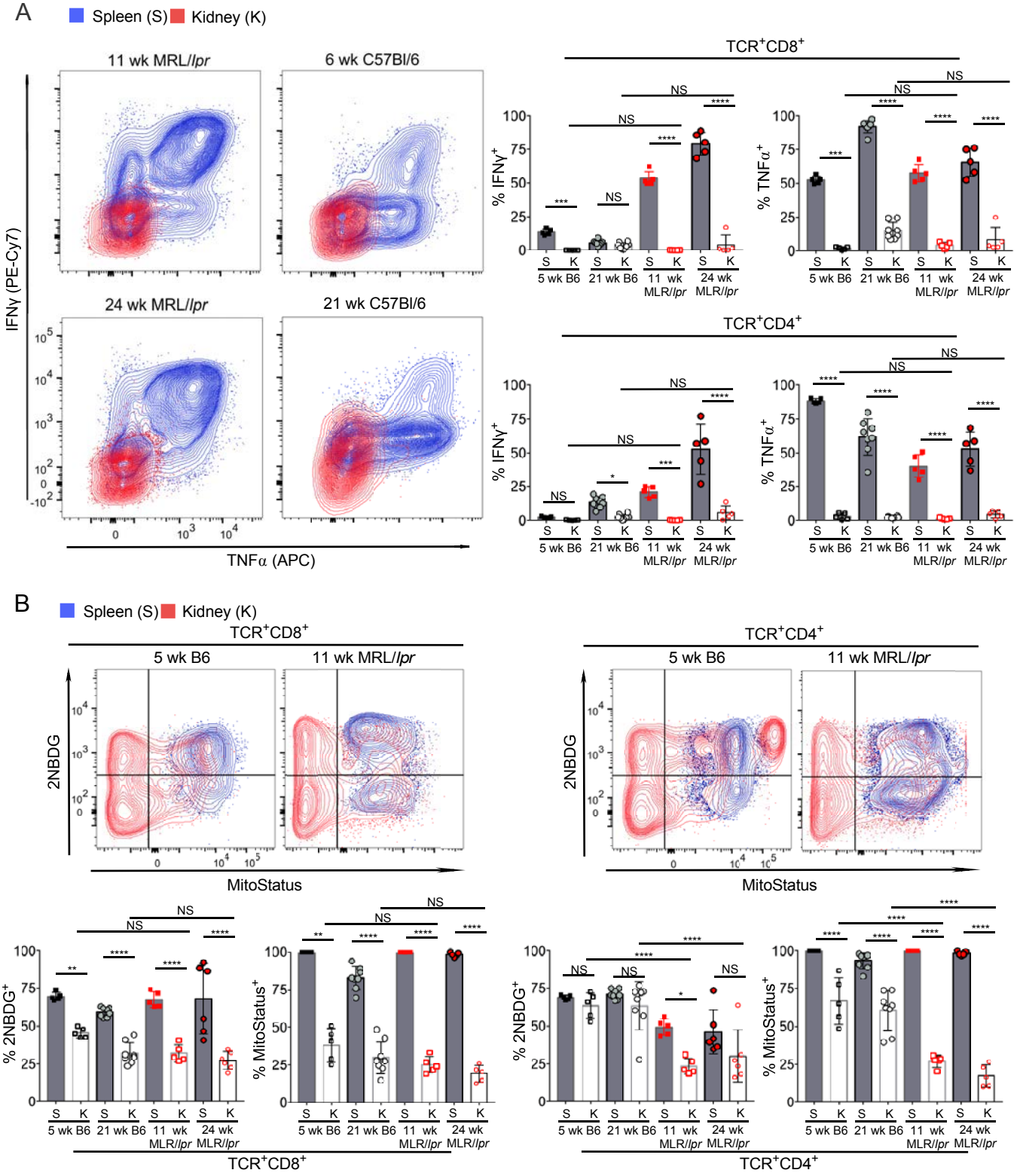

Supplemental Figure 3: Kidney-infiltrating T cells from lupus and non-lupus prone mice have reduced cytokine production and altered metabolic profile.

(A) T cells were isolated from the kidney (red) and spleen (blue) of indicated strains (aged and young B6 and MRL/*lpr* mice). Bulk culture was stimulated with PMA and ionomycin in the presence of brefeldin A for 4 hours and cytokine expression was assessed by flow cytometry.

Representative contour plots show cytokine production by CD8$^+$ T cells from indicated strains (left panels). Summary data panels (right) represent frequency of positive cells. Grey bars (S) indicate splenic T cells and white bars (K) indicate KITs from labeled mouse strains.

(B) Representative contour plots of indicated strains showing 2-NBDG (glucose uptake) and MitoStatus (mitochondrial membrane potential uptake) in matched KITs (red) and splenic T cells (blue) in both the CD8+ (left panel) and CD4+ (right panel) T cell compartments. Summary data represents frequency of positive cells. Grey bars (S) indicate splenic T cells and white bars (K) indicate KITs from labeled mouse strains.

For summary data (A,B) Each dot denotes an individual mouse with bars representing the mean and error bars showing 1 standard deviation. Young B6 (n=5), aged B6 (n=9), young MRL/*lpr* (n=5), aged MRL/*lpr* (n=5), represent mice combined from several experiments in a single analysis. ANOVA with Tukey's multiple comparison test was used to determine statistical significance between all samples (* p<0.05, ** p<0.01, *** p<0.001,**** p<0.0001).

Supplemental Figure 4

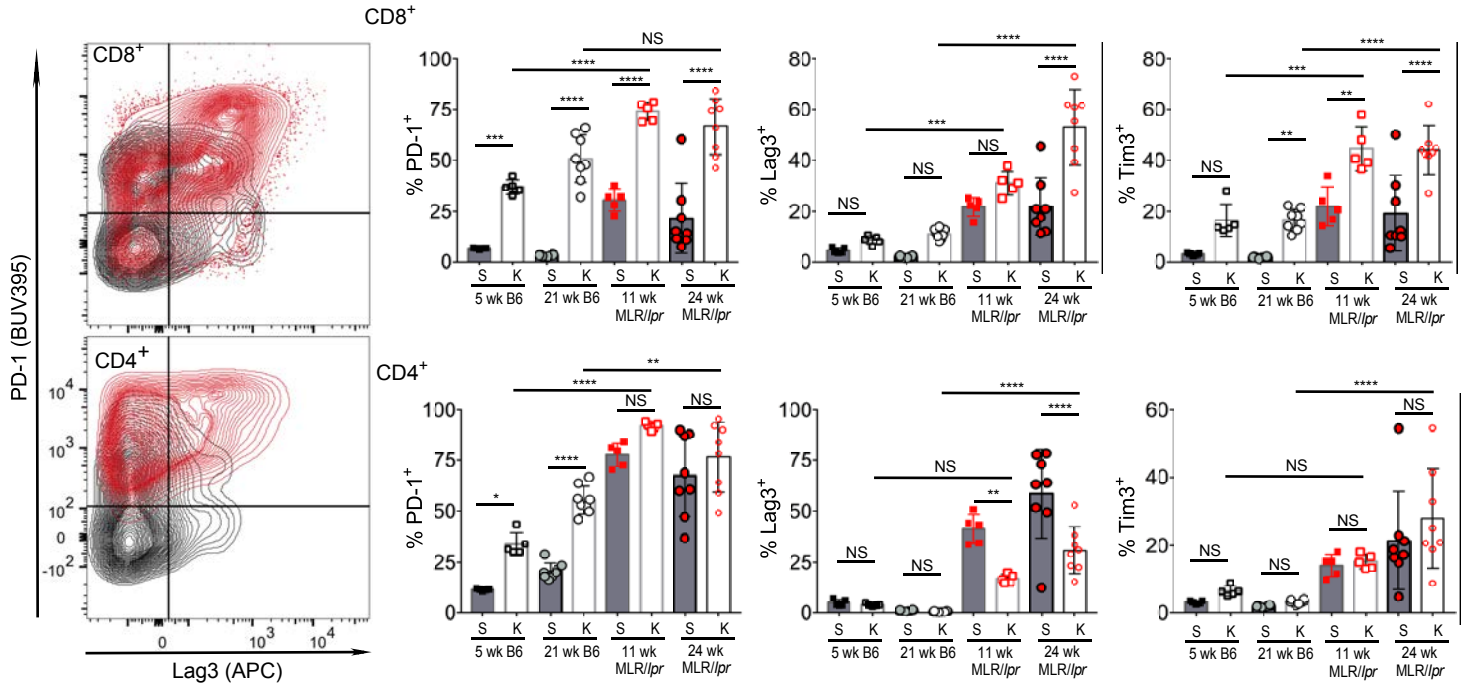

Supplemental Figure 4: Inhibitory receptors are increased in KITs compared to splenic T cells.

(A) Representative contour plots of CD8$^+$ T cells from 6 week old B6 KITs (black) and 11 wk MRL/*lpr* KITs (red) depicting expression of exhaustion markers PD-1 and Lag 3.

(B) Tabulated data of the frequency of IR expression on CD4$^+$and CD8$^+$ T cells. Grey bars (S) indicate splenocytes and white bars (K) indicate KITs from indicated mouse strains. Each dot denotes an individual mouse with bars representing the mean and error bars showing 1 standard deviation. Young B6 (n=5), old B6 (n=9), young MRL/*lpr* (n=5), old MRL/*lpr* (n=8) represent mice combined from several experiments in a single analysis. ANOVA with Tukey's multiple comparison test was used to determine statistical significance between spleen and kidney samples (* p<0.05, ** p<0.01, *** p<0.001,**** p<0.0001).

Supplemental Figure 5

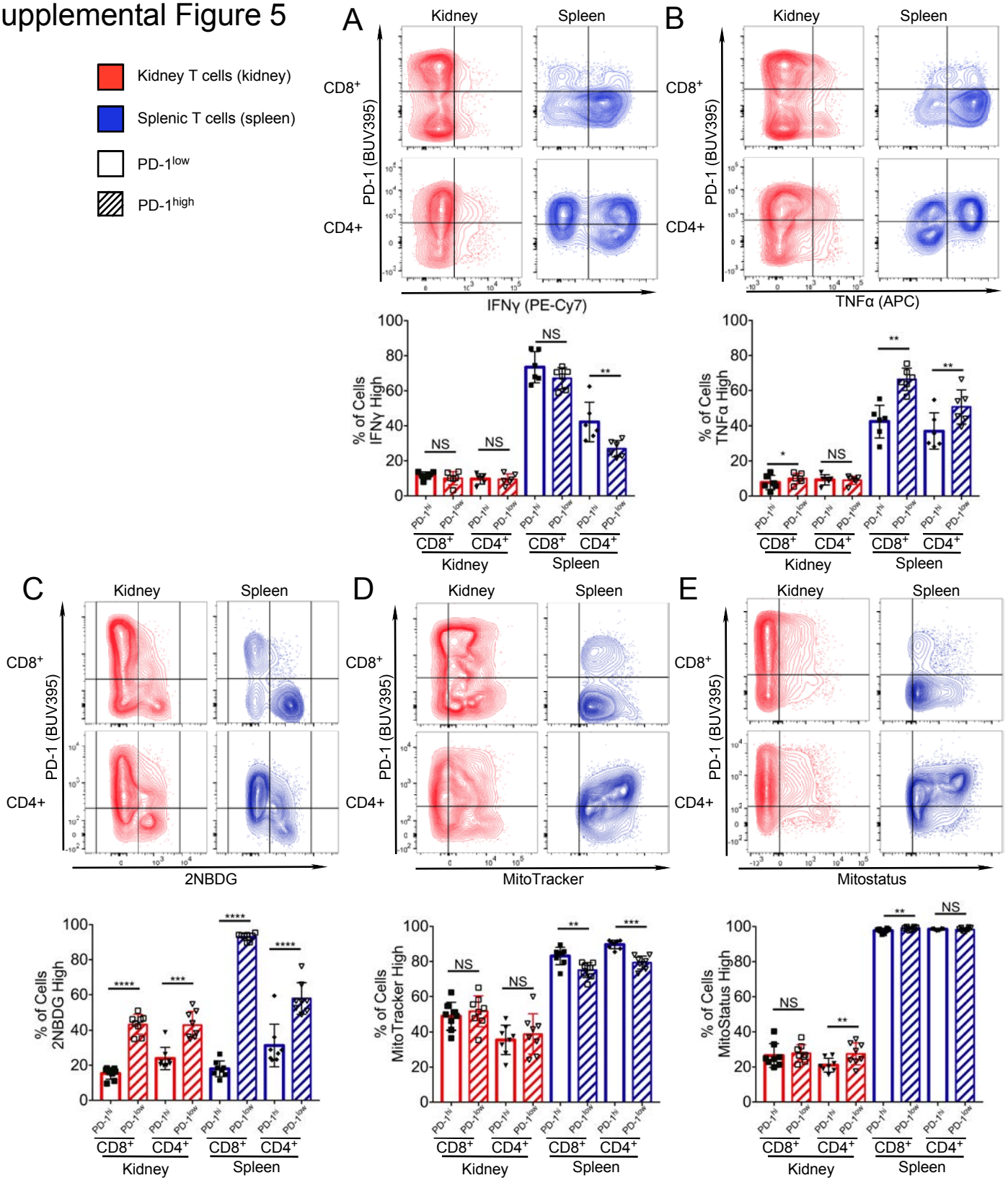

Supplemental Figure 5. PD-1 expression in MRL/*lpr* mice correlates with glucose uptake but not other metabolic markers in KITs.

(A-E) Representative contour plots of expression of PD-1 vs. the indicated cytokine or metabolic marker for the T cell lineage and tissue indicated. Bar graphs show the percentages of $CD4^+$ or $CD8^+$ T cells, categorized by either high or low expression of PD-1, that express: (A) IFNγ (n=6), (B) TNFα (n=6), (C) 2-NBDG (n=8), (D) MitoTracker (n=6), and (E) MitoStatus (n=6). For tabulated data each dot denotes an individual mouse with bars representing the mean +/- 1 standard deviation. A paired Student's t test was used to determine statistical significance between spleen and kidney samples and PD-1 high and low populations (** $p<0.01$, *** $p<0.001$,**** $p<0.0001$).

Supplemental Figure 6

A

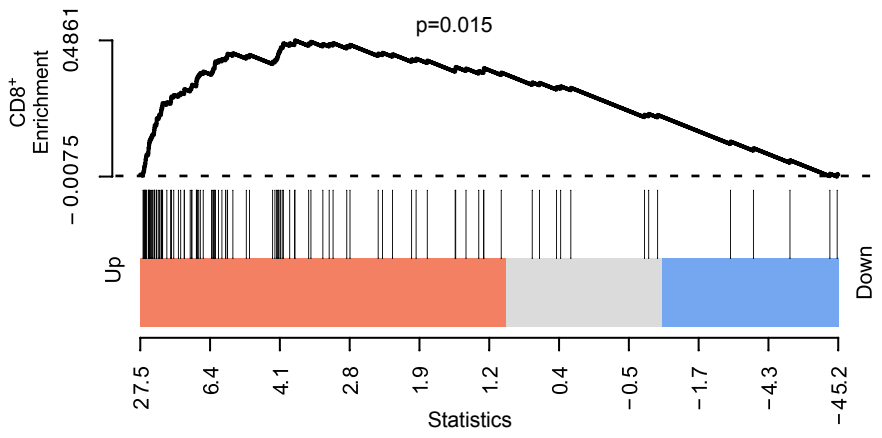

B

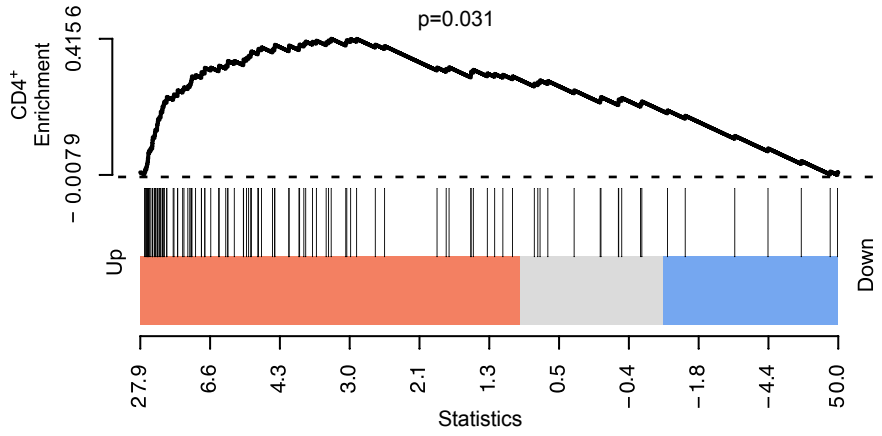

Supplemental Figure 6. Genes associated with LCMV induced exhaustion are enriched in KITs derived from MRL/*lpr* mice.
GSEA plots evaluating enrichment of 105 LCMV induced exhaustion related genes (37) among genes differentially regulated between kidney and splenic derived T cells (n=3 per group) are shown for both $CD8^+$ (A) and $CD4^+$ (B) compartments. P-values were calculated using the “rankSumTestWithCorrelation” function in the limma package.

Supplemental Figure 7

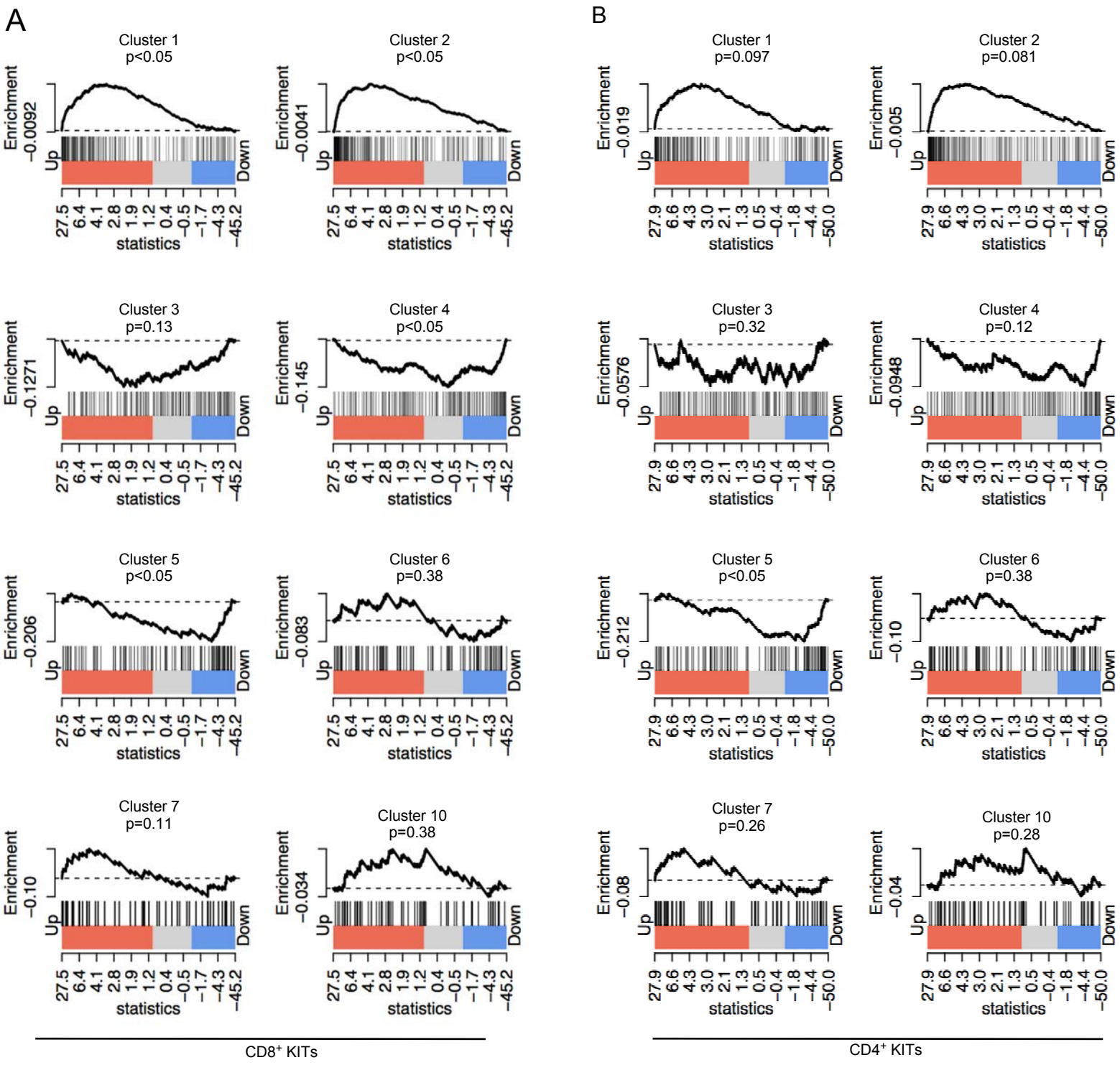

Supplemental Figure 7. Shown are GSEA plots evaluating enrichment of 8 of 10 predefined gene set clusters derived from melanoma tumor infiltrating T cells (TILs) compared to naïve controls (36) among regulated genes differentially expressed between KITs and splenic T cells of MRL/*lpr* mice. (A) $CD8^+$ and (B) $CD4^+$ cell analysis (n =3 per group). Clusters C1 and C2 are associated with PD-1^+ $Tim3^+$ TILs (commonly linked with exhaustion) while clusters C3, C4, and C5, C6 are associated with phenotypically naïve or effector populations respectively. Clusters C7, C10 are also associated PD-1^+ $Tim3^+$ TILs and to a lesser extent effector populations. P-values were calculated using the "rankSumTestWithCorrelation" function in the limma package. The number of genes assessed is as follows, cluster 1 (176 genes), cluster 2 (272 genes), cluster 3 (203 genes), cluster 4 (226 genes), cluster 5 (109 genes), cluster 6 (90 genes), cluster 7 (45 genes), and cluster 10 (68 genes).

Supplemental Figure 8

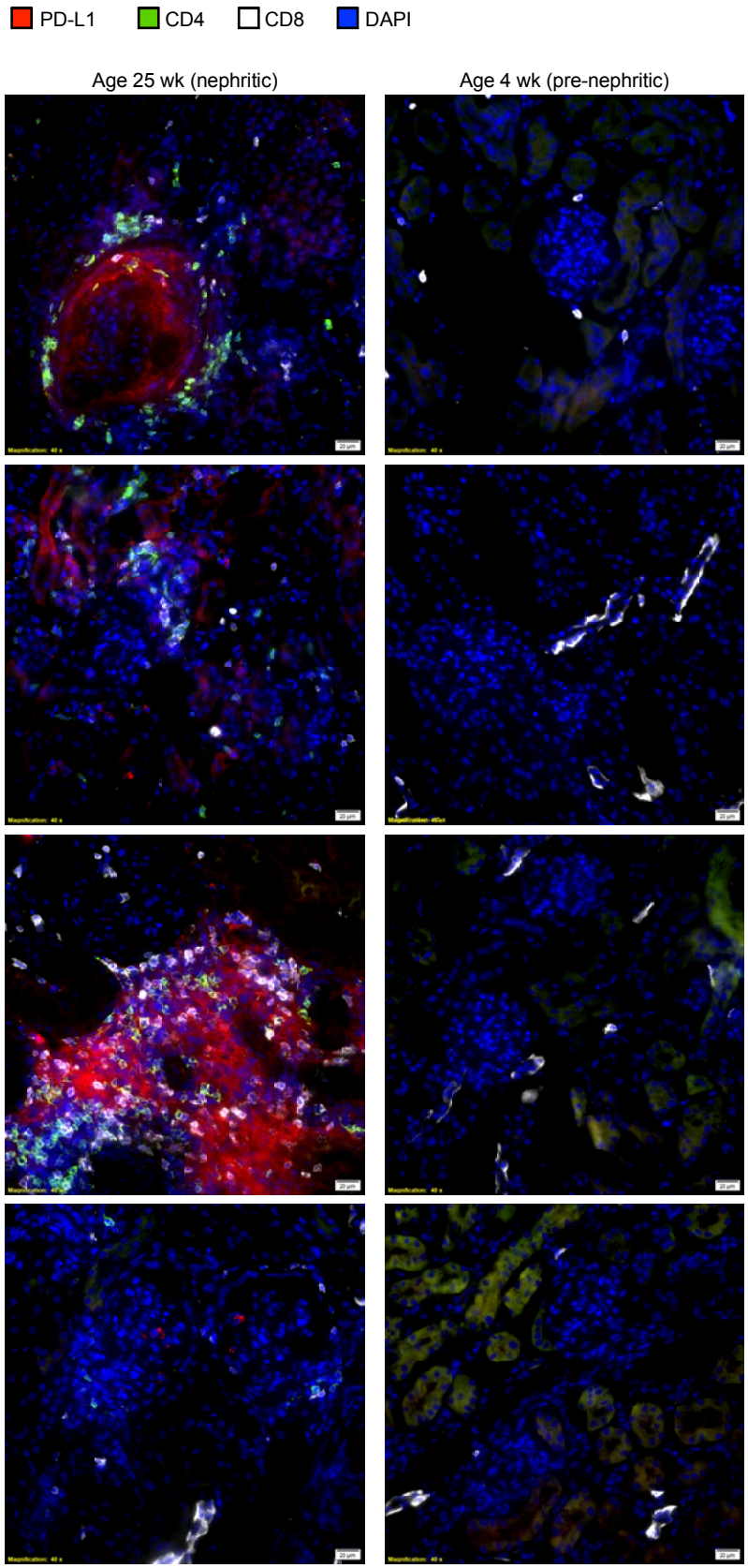

Supplemental Figure 8. MRL/*lpr* nephritic kidneys express PD-L1 near sites of T cell infiltrates. Frozen sections from nephritic (aged >20 weeks) or pre-nephritic (4 weeks) MRL/*lpr* kidneys were stained by immunofluorescence for $CD4^+$ (green), $CD8^+$ (white), and PD-L1 (red) expression with DAPI (blue) to mark nuclei. These images represent 4 additional animals from each group, stained as outlined in Figure 6. Images were set to a standard threshold and capture time for PD-L1 for comparison purposes. Representative images are shown at 40x magnification.

Supplemental Figure 9

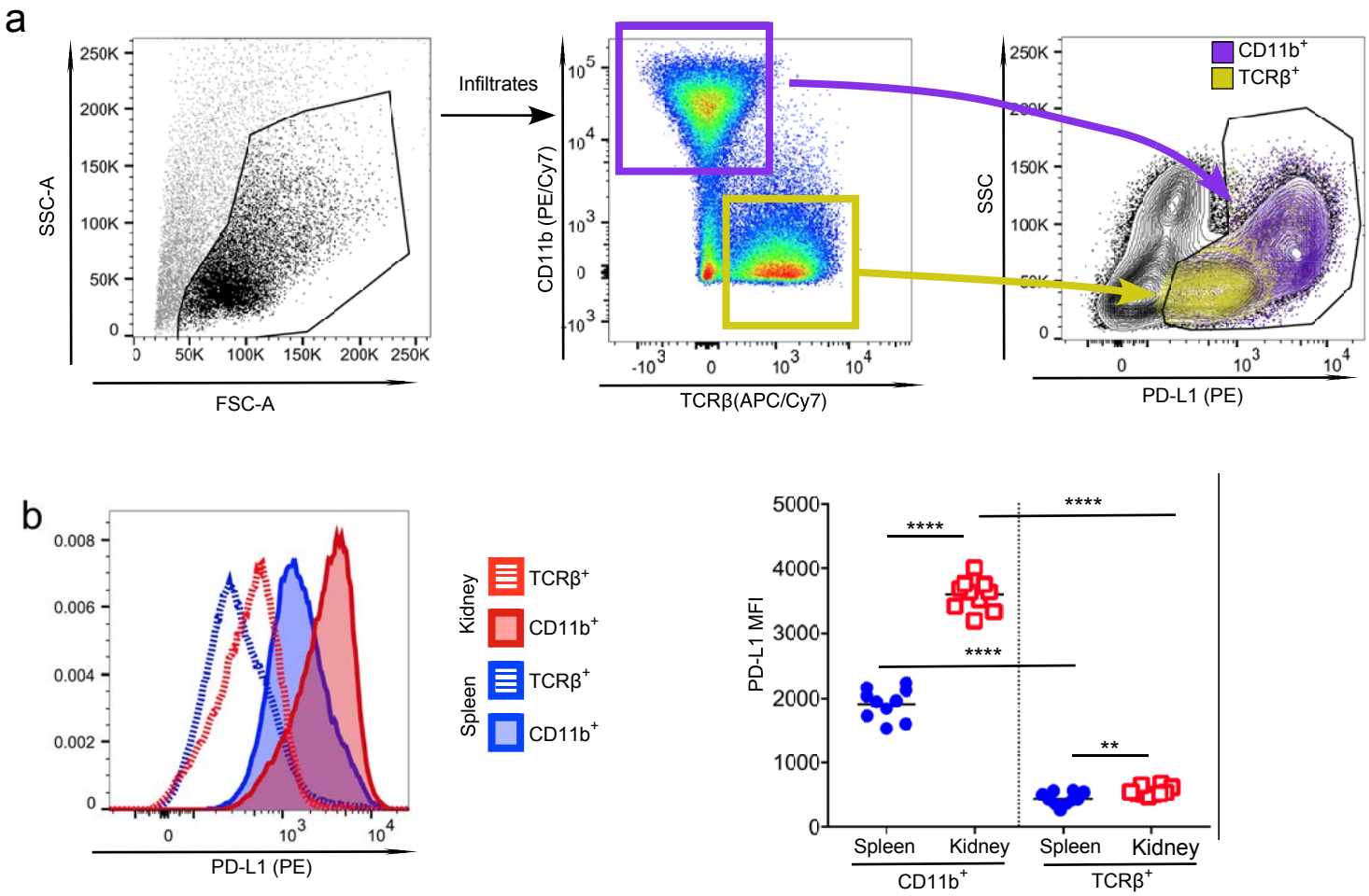

Supplemental Figure 9. Kidney-infiltrating CD11b$^+$ cells from MRL/*lpr* mice exhibit increased amounts of PD-L1 expression**.**

(A) Gating strategy to define PD-L1$^+$ kidney-infiltrating cell populations. Gating was first on the infiltrating population from total kidney single cell population (left panel), then CD11b$^+$ and TCRβ$^+$ subpopulations within the infiltrating population (middle panel), and then PD-L1 expression of defined CD11b$^+$ and TCR$^+$ infiltrating subpopulations was plotted (right panel).

(B) PDL-1 expression on spleen and kidney T cells (red) and myeloid cells (blue). Representative histogram (left) and summary data of PD-L1 MFI (right). This experiment was performed as a single technical replicate on 10 mice. For tabulated data each dot denotes an individual mouse, horizontal lines represent the mean with error bars representing one standard deviation. A paired Student's t test was used to determine statistical significance between spleen and kidney samples and hematopoietic subpopulations (** $p<0.01$, **** $p<0.0001$).

Supplemental Figure 10

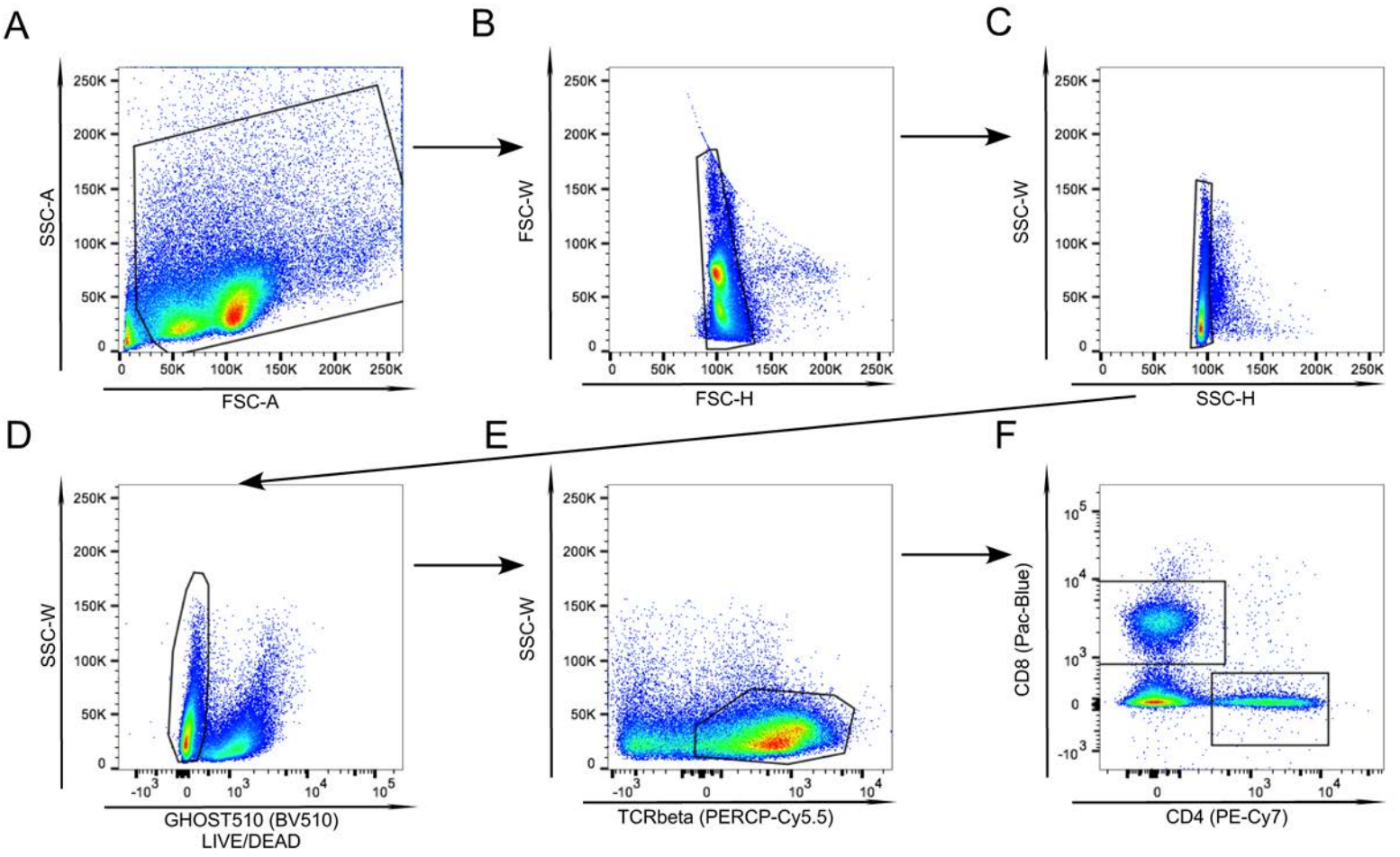

Supplemental Figure 10. Generalized gating strategy for splenic T cells.
Lymphoid cells were gated according to their FSC-A/SSC-A profile (A) to exclude debris. The doublets corresponding to cell aggregates were also excluded by the FSC-W/FSC-H profile (B) and SSC-W/SSC-H (C). Single cells (in gate G2) were subsequently gated on live cells (D). For the majority of studies in this manuscript live cells were then gated on TCRβ$^+$ cells (E) followed by CD4$^+$ and CD8$^+$ populations (F).